In-Situ Cu-based Bulk Metallic Glass Composites

H. Wang[1], H. M. Fu[1,2], H. F. Zhang[2], Z. Q. Hu[2]
1 School of Engineering, The University of Queensland, St Lucia, QLD 4072, Australia
2 Shenyang National Laboratory for Materials Science, Institute of Metal Research, Chinese Academy of Sciences, Shenyang, 110016, China

Cu-based bulk metallic glasses are of relative low cost and high strength. They have more potential to be used as engineering materials. However, the lack of ductility has largely limited their applications. In the last few years, attempts have been made to form Cu-based BMG composites with two-phase microstructure to improve the ductility of BMGs, including extrinsic composites, in-situ composites and nanocrystalline composites. In this paper, two *in-situ* BMG composites have been successfully prepared with TiC and TiB particles respectively *in-situ* formed in the Cu-based BMG matrix. After the introduction of the TiC and TiB particles, besides of the lineal increase of hardness, the materials exhibit significant plasticity.

Key words: Bulk metallic glasses; BMG composites; Cu-based BMG; Ductility

1. Bulk Metallic Glasses and Bulk Metallic Glass Composites

The last decade has seen the discovery of bulk metallic glasses (BMGs) that are amorphous alloys produced in the bulk via conventional metal processing such as casting, but with the ease of molding of polymers[1-4]. BMGs receive a great attention as a new class of structural materials because of their excellent properties such as high strength, great elasticity and good corrosion and wear resistances. The mechanical properties of BMGs bulk metallic glasses are in many cases superior to their crystalline counterparts[5,6]. The tensile strength of BMGs is very high (σ_y >2 GPa, even 5 GPa[7] was reported in some alloy systems), and the elastic strain limit is about 2%, much higher than common crystalline metallic alloys (<1%). BMGs also exhibit good fracture toughness (>55 MPa m$^{1/2}$) and very good hardness. Very high strength (also specific strength, σ/ρ) and high elastic limit make BMGs excellent candidates for structural applications. However, all the BMGs discovered so far exhibit very limited plasticity[8]. Under a tensile loading condition, BMGs fail catastrophically on one dominant shear plane and show little global plasticity. On the contrary, under a compressive loading condition, BMGs tend to form several shear bands but the propagation of the shear bands is localised in a very narrow region to accommodate the plastic strain. The localised deformation causes strain softening or thermal softening in the shear bands. The failure of the BMGs occurs typically along a single shear band that cuts across the sample at an angle of 45° to the applied stress, which is the direction of maximum resolved shear stress[9].

In the last few years, attempts have been made to form bulk metallic glass matrix composites with a two-phase microstructure to improve the ductility of BMGs. Here the amorphous BMG acts as the matrix and a crystalline-phase reinforcement material acts both as initiation sites for shear bands and as barrier to shear band propagation[10]. Multiplication, branchinv and restriction of the shear bands lead to ductility enhancement. There are three types of BMG composites[10]: (1) in-situ BMG composites, in which primary dendrites or particles are formed in a well designed alloy composition during solidification; (2) extrinsic BMG composites, in which external reinforcement is added into a BMG matrix; and (3) nanocrystalline BMG composites, in which nanocrystals are precipitated through annealing of BMG precursors. The two-phase BMG matrix composite combines the high strength of the monolithic BMG with the advantages of crystallinity, i.e. increased ductility, fracture toughness and plastic strain-to-failure.

2. *In-situ* Bulk Metallic Glass Composites

In a well-designed alloy system, through controlled crystallization, the ductile phase may be *in-situ* precipitated while the remaining liquid solidifies as a bulk metallic glass. The precipitates can be either ductile dendrites or brittle particles. The *in-situ* formed precipitates promote generation of multiple shear bands and restrict shear band propagation. They are also possible to create other propagation directions for the shear band, which are different from the direction of the maximum shear stress.

For the *in-situ* BMG composites, the alloy composition is critical, because on one hand the melt needs to be able to partially crystallize to form the chosen reinforcements upon cooling; on the other hand, crystallization needs to be suppressed in the rest of the melt in order to form BMG as the matrix. To design the *in-situ* BMG composites, Different BMG systems have different composition and crystalline structure for the reinforcement phases. There are already several successful reports on the *in-situ* BMG composites.

In Zr-based BMGs, Johnson's group[11] reported *in-situ* composite that, upon cooling the composition in the neighborhood of Vit1 ($Zr_{56.2}Ti_{13.8}Nb_5Cu_7Ni_{5.5}Be_{12.5}$), a micrometer-sized ductile β-ZrTi, with body-centered cubic (bcc) structure, precipitated and shifted the composition of the remaining liquid close to that of Vit1, so the remaining liquid solidified as a bulk metallic glass. The element Nb was added to stabilize the ductile bcc phase over the α-ZrTi (hcp) phase. The resulting two-phase microstructure effectively modified shear band formation and propagation. A high density of multiple

shear bands evolved upon loading, which resulted in a significant increase of ductility both in tension and compression, toughness, and impact resistance compared to the monolithic glass. The overall (tensile and compressive) plastic strain of this in situ composite was about 5%. Das[12] et al. also reported similar results and successful preparation of Be-free *in-situ* Zr-based BMG composites with mico-scale ductile bcc phase reinforcement.

In the Ti-based BMGs, He et al. reported [13] *in-situ* composite with ductile β-Ti(Ta, Sn) dendritic precipitated (hexagonal close-packed (hcp)). The ductile dendritic hcp-Ti solid solution dispersing in the glassy/nanocrystalline matrix increased plasticity and fracture strength of the composites. The material exhibited up to 14.5% compressive plastic strain.

3. *In-situ* Cu-based BMG composites

Cu-based BMGs become more attractive for the applications as structural materials because of their relative low cost and high strength. There are increasing interests in recent years in the development of Cu-based BMGs with improved ductility. In this study, we have investigated two *in-situ* Cu-based BMG composites.

3.1 TiC-contained in-situ Cu-based BMG composites

$Cu_{47}Ti_{33}Zr_{11}Ni_6Sn_2Si_1$ was chosen as the BMG matrix due to its strong glass forming ability. BMG rod with a diameter of 6 mm has been reported in this alloy system[14]. TiC particle was designed as the reinforcement phase. C was added as a form of Ni-C master alloy. $(Cu_{47}Ti_{33}Zr_{11}Ni_6Sn_2Si_1)_{100-x}C_x$ alloys were prepared by arc melting of a mixture of the BMG component elements and the master alloy. The alloys were then remelted in a quartz tube by induction melting, followed by casting into copper moulds with cylindrical cavity of diameter 2.5 mm[15].

Fig.1 shows the XRD patterns for the as-cast monolithic Cu-based BMG and the BMG composite. The monolithic BMG only exhibits a characteristic broad diffraction of metallic glass with no evidence of any crystalline Bragg peaks, indicating the formation of a single amorphous phase. While for the BMG composite, sharp crystallization peaks are observed on the top of the broad halo diffraction of the amorphous phase. The position and intensity of the crystalline peaks match exactly with that of titanium carbide. The EDS results also confirm the crystalline particles contain only titanium and

carbon elements. No other phases are detected within the sensitivity limits of the XRD. The results indicate that the addition of carbon induce the formation of TiC particles during solidification, while the remaining liquid solidifies as amorphous phase due to its high glass-forming ability.

Fig. 2 shows the optical micrographs of the BMG composite containing 3.6, 15.2 and 26.8 vol.% TiC. TiC particles embedded in the amorphous matrix are uniformly distributed. The average size of TiC particles is about 4 μm. When the volume fraction of TiC increases, the particles exhibit some extent of agglomeration with particles gather together forming particle groups. Neither pores nor voids appear over the whole cross section of the samples. SEM microstructure analysis confirms a true bonding state existing at the interface between the amorphous matrix and TiC reinforcement.
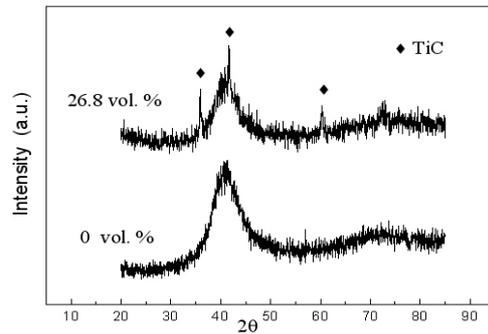
Fig.1   XRD patterns of Cu-based BMG and BMG composite containing 26.8 vol.% TiC particles

Fig.3 shows the DSC curves for the Cu-based BMG and BMG composites. They all show a similar pattern with an apparent glass transition followed with a three-step crystallization process. The existence of TiC seems has no significant effect on the glass transition temperature (T_g). However, the initial crystallization temperature T_x moves to a higher temperature with the increase of TiC volume fraction, therefore the supercooled liquid region (ΔT) increases. ΔT was 53K for the monolithic BMG and gradually increased to 62K for alloy with 26.8 vol.% TiC. The increase of the supercooled liquid region is an indicator of the increase of thermal stability. This might because some small carbon atoms introduced to the system dissolve into the BMG matrix, which further increase the complexity of the BMG structure. Increasing the TiC volume fraction also leads to the second and the third crystalline peaks moving to lower temperatures.
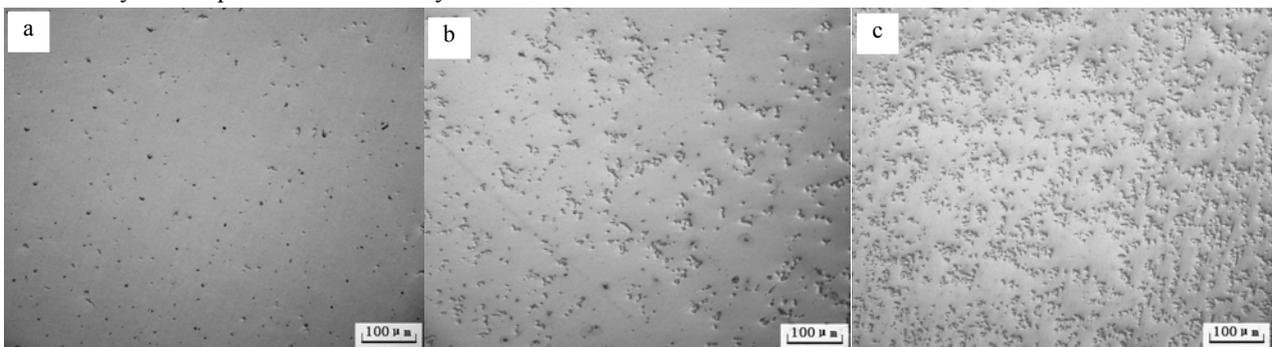
Fig.2 Optical micrographs of the Cu-based BMG composites containing (a) 3.6 vol.%, (b) 15.2   vol.% and (c) 26.8 vol. % TiC particles
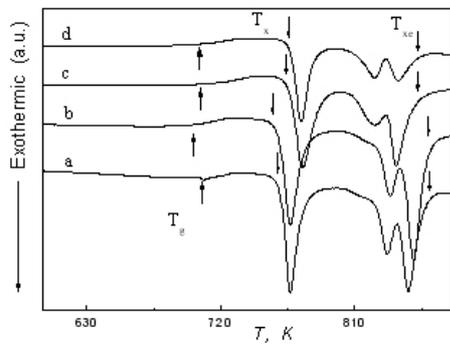
Fig.3 DSC curves of Cu-based BMG and BMG composites: (a) 0 vol.%; (b) 3.6 vol.%, (c) 15.2 vol.% and (d) 26.8 vol.% TiC

Fig.4 shows the compressive stress-strain curves of the Cu-based BMG and BMG composites. In general, the compressive fracture takes place along the maximum shear plane, which is inclined by about 45° to the direction of applied load. It can be seen that the monolithic Cu-based BMG has the compressive fracture strength of 2250 MPa, but with no plastic deformation. For the BMG composite containing 3.6% TiC, the fracture strength is similar, but the material exhibits obvious compressive plastic deformation after yielding. Its plastic strain is about 0.6%. Further increasing the TiC volume to 15.2% results in a decrease in the plastic strain, but the fracture and yield strength reach to maximum values of 2500 MPa and 2210 MPa respectively. When the TiC volume reaches to 26.8%, both fracture strength and plastic strain decrease, and the material exhibits the similar fracture properties of the monolithic BMG. It should be noted that the fracture strength of the all BMG composites is also higher than that of the other Cu-based monolithic BMGs which have been reported: 2040 MPa for Cu-Ti-Zr-Ni-Si alloy and 2186MPa and for Cu-Ti-Zr-Ni alloy[16].

Table.1 summarizes the mechanical properties of Cu-based BMG composites containing varying volume fraction of TiC particles. It should be noted that the hardness of the materials continuously increases with the increase of the volume fraction of TiC particles, from Hv543 for the monolithic BMG to Hv 681 for the 26.8 vol.% BMG composite, enhanced by 25%.

Figs. 5 shows the fracture surface of the BMG composites. In the 3.6% TiC sample, except the vein-patterns, which are the classical characteristics of fracture surface of BMGs, honeycomb-like holes are observed on the fracture surface (Fig.5(a)). The honeycomb-like fracture pattern might be the cause of good ductility in the material. In the 15.2% TiC sample, the vein patterns disappear (Fig.5(b)). TiC particles are observed uniformly distributed on the fracture surface. Shear bands propagate and stop at the particles. The suppression of the shear band propagation by the TiC particles results in a higher strength. Further increasing the TiC fraction to 26.8 vol.% TiC, the particles tend to group as can as particle clusters, as shown in Fig.2(c). Such particle clusters can also be observed on the fracture surface (Fig.5 (c)), and cracks often appear at the points of particle agglomeration, indicating that the joint area of the particles might serve as the origin of the cracks under loading. More liquid metal droplets are observed on the fracture surface of the high TiC-contained sample.

Table.1 Mechanical properties of Cu-based BMG and BMG composites containing TiC particles

TiC, vol%	Yield strength (MPa)	Fracture strength (MPa)	Plastic strain %	Vicker's hardness (HV)
0	1930	2250	0	543
3.6	1910	2200	0.6	551
15.2	2210	2500	0.2	605
36.8	2050	2160	0	681
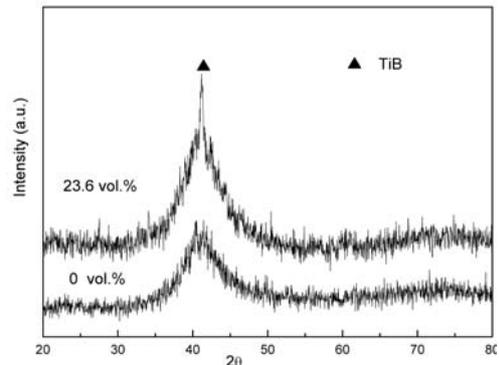
Fig.6 XRD patterns of Cu-based BMG and TiB-contained BMG composite.

Fig.5 Fracture surface of Cu-based BMG composites containing: (a) 3.6 vol %, (b) 15.2 vol% and (c) 26.8 vol.% of TiC particles.
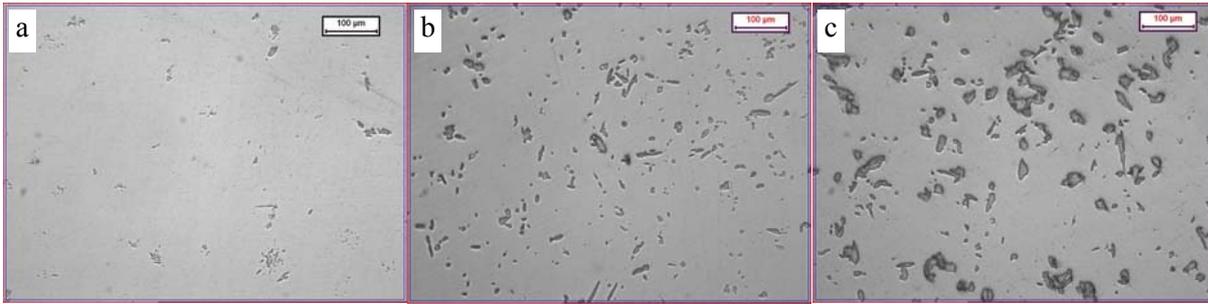
Fig.7 Optical micrographs of Cu-based BMG composites containing (a) 5.2, (b) 17.5 and (c) 23.6 vol. % TiB particles

3.2 TiB-contained in-situ Cu-based BMG composites

$Cu_{47}Ti_{33}Zr_{11}Ni_6Sn_2Si_1$ was also chosen as the BMG matrix. B was added as a form of Ni-B master alloy. During solidification TiB was in-situ formed from the melt. TiB particles reinforced Cu-based BMG composites were obtained by the same way as for the TiC reinforced BMG composites. Fig. 6 shows the XRD pattern of the TiB-contained BMG composite. Sharp TiB crystalline peak were observed on the top of the broad holo diffraction. The EDS results confirmed the crystalline phase is TiB.

Fig.7 shows the microstructure of TiB-contained BMG composites. The volume fractions of TiB particles are 5.2, 17.5 and 23.6 vol. % respectively. The TiB particles are relatively uniformly distributed in the amorphous matrix. The particle size increases slightly with the increase of the TiB volume. In the 23.6% TiB sample, the average particle size is about 8 μm. SEM analysis verifies that the materials have a very good bonding between the amorphous matrix and reinforcing particles.

Table 2 Mechanical properties of TiB-contained
Cu-based BMG composites

TiB, vol.%	Vicker's hardness (HV)	Yield strength (MPa)	Fracture strength (MPa)	Plastic strain (%)
0	543	1930	2250	0
5.2	560	2060	2523	0.5
17.5	610	2019	2575	2
23.6	650	2008	2363	0.5

Table 2 summarizes the mechanical properties of BMG composites reinforced by TiB. With increasing the volume fracture of TiB particles, the hardness of the BMG composites lineally increases from Hv 543 for the non-TiB sample to Hv 650 for the 23.6% TiB-enhanced composite. The results from the compressive test show that fracture strength also increases with the introduction of TiB. It reaches to the maximum with a strength of 2575 MPa for the 17.5 vol% TiB sample. More significantly, the BMG composite exhibits obvious plasticity with a plastic strain of 2 %. The plasticity is shown in all composite samples.

More recently, Cu-based BMG composites containing *in-situ* precipitated ductile dendrites have been reported. An *in-situ* formed composite with Ta-rich solid solution particles precipitated from $(Cu_{60}Zr_{30}Ti_{10})_{95}Ta_5$ alloy exhibited plastic strain to failure of about 14.5%[17]. In another alloy system, a Nb-rich phase was *in-situ*

formed in $(Cu_{60}Zr_{25}Ti_{15})_{93}Nb_3$ and plastic strain reached to 6.4%[18]. Another recent interesting development was from Das et al. which reported that a monolithic BMG $Cu_{47.5}Zr_{47.5}Al_5$ exhibited a ductility of 18%[19].

4. Summary

Cu-based BMGs are relatively of low cost and high strength. Forming BMG composite has been proven as an successful approach to enhance ductility of the materials. Two *in-situ* BMG composites have been successfully prepared with TiC and TiB particles respectively in-situ formed in the Cu-based BMG matrix. After the introduction of the TiC and TiB particles, besides of the lineal increase of hardness, the materials exhibit significant plasticity.

References
1. A.Inoue, T.Zhang and T.Masumoto, Mater. Trans. JIM, 1989, 30, 965.
2. A.Inoue, K.Ohtera, K.Kita and T.Masumoto, *Japan J. Appl. Phys.,* 1988, 27, L2248.
3. A.Peker and W.L.Johnson, *Appl. Phys. Lett.*, 1993, 63, 2342.
4. W.H.Wang, C.Dong and C.H.Shek, Mater. Sci. & Eng. 2004, R44, 45.
5. W.L.Johnson, JOM, 2002, 40, 54**.**
6. A.Inoue, *Acta Mater.*, 2000, 48, 279.
7. A.Inoue, B.L.Shen, H.Koshiba, H.Kato and A.R. Yavari, 2004, 52, 1631.
8. A.L.Greer, Scienc, 1995, 267, 1947.
9. E. Pekarskaya, C.P. Kim and W.L. Johnson, J. Mater. Res., 2001, 16, 2513.
10. H.Wang, J. Mater. Sci. & Tech., 2005, 21, suppl.1, 86.
11. C.C.Hays, C.P.Kim and W.L.Johnson, Phys. Rev. Lett., 2000, 84, 2901.
12. J. Das, W.Loser, J.Eckert, S.K.Roy and L.Schultz, Appl. Phys. Lett., 2003, 82, 4690.
13. G.He, J.Eckert, W.Loser and L.Schultz, Nature Materials, 2003, 2, 33.
14. E.S.Park, H.K.Lim, W.T.Kim and D.H.Kim. J Non-Cryst Solids, 2002,15. 298.
15. H.Fu, H.Zhang, H.Wang, Q.Zhang and Z.Q.Hu, Scripta Materialia, 2005, 52, 669.
16. M.Calin, J. Eckert, L. Schultz. Scripta Mater, 2003, 48, 653.
17. Y.C.Kim, D.H. Kim and J.C. Lee, Mater. Trans. JIM, 2003, 44, 2224.
18. Z.Bian, J.Anhmad, W.Zhang and A.Inoue, Mater. Trans. JIM, 2004, 45, 2346.
19. J.Das, M.B.Tang, K.B.Kim, R.Theissmann, F.Baier, W. H.Wang and J.Eckert, Phys. Rev. Lett., 2005, 94, 205501.